Available online at www.sciencedirect.com

ScienceDirect

Procedia Engineering 105 (2015) 919 – 927

Procedia Engineering

www.elsevier.com/locate/procedia

6th BSME International Conference on Thermal Engineering (ICTE 2014)

Blood Flow Dynamics in Cerebral Aneurysm - A CFD Simulation

Shamiul Sarkar Shishir[a], Md. Abdul Karim Miah[a], A K M Sadrul Islam[a], and A B M Toufique Hasan[b]

[a] Department of Mechanical and Chemical Engineering, Islamic University of Technology (IUT), Board Bazar, Gazipur-1704, Bangladesh

[b] Department of Mechanical Engineering, Bangladesh University of Engineering and Technology (BUET), Dhaka-1000, Bangladesh

Abstract

In the present study, the dynamics of blood flow in saccular cerebral aneurysms is investigated. The aneurysm is considered to be located at an arterial bend in human vascular system. The flow field is analyzed computationally by three-dimensional Navier-Stokes equation for laminar flow of incompressible Newtonian fluid. Circular and elliptical necks of different sizes are studied. The vascular wall is considered rigid for simplicity. Hemodynamic parameters such as velocity, pressure, vortices, wall shear stress and so on are considered for characterization of flow field. Results showed that the vortex location, inflow area in the neck and so on are varied significantly with the geometrical parameter of the aneurysm.

Peer-review under responsibility of organizing committee of the 6th BSME International Conference on Thermal Engineering (ICTE 2014)

Keywords: Aneurysm; Blood Flow; CFD.

1.Introduction:

Cerebral aneurysms (also called brain/intracranial aneurysms) are a cerebrovascular tissue in which weakness in the walls of a cerebral artery causes localized dilation or ballooning in the blood vessel.

Corresponding author. Tel.: +880-01739103922;
E-mail address: shishir2180@gmail.com

Peer-review under responsibility of organizing committee of the 6th BSME International Conference on Thermal Engineering (ICTE 2014)
doi:10.1016/j.proeng.2015.05.116

Over time, the blood flow within the artery pounds against the thinned portion of the wall and aneurysms form silently from wear and tear on the arteries. As the artery wall gradually becomes thinner from the dilation, the blood flow causes the weakened wall to swell outward. This pressure may cause the aneurysm to rupture and allow blood to escape into the space around the brain which is called hemorrhage.

Subarachnoid hemorrhage (SAH) is a highly lethal condition with a 30-day mortality rate of 45%. About 15% of patients die before reaching the hospital. 40% will not survive the first two weeks despite the best available care. Of the remaining 60%, more than half will be permanently disabled, perhaps 20% will return to their pre-rupture employment and level of function.

Saccular aneurysm is the most common type of aneurysm accounting for 80-90% of all intracranial aneurysms and are the most common cause of non-traumatic subarachnoid hemorrhage (SAH). This type looks like a sac or berry forms at the bifurcation of the arteries and branches of the large arteries at the base of the brain, known as the circle of willis [1].

Loading (wall stress) and the mechanical properties of arterial wall are the predominant factors for rupture of aneurysm. Wall stress is mainly dependent on mechanical properties of arterial wall, aneurysm geometry and aneurysm pressure [2]. Shear stress inside the aneurysm alters permeability of arterial wall and transport between lumen and wall. Because of hemodynamic change, endothelial cells activate the biochemical factors controlling the adaptation of arterial wall. This adaptation may degrade and weaken arterial wall resulting in aneurysm growth. If the stress exceeds the strength the rupture takes place.

Hoi et al. [3] suggests that risk of aneurysm growth increases with larger arterial curvature and aneurysm neck size for variable curvature. Sato et al [4] examined lateral saccular aneurysm models with different aneurysm shapes (i.e., the ratio of aneurysm height to aneurysm neck diameter) and different configurations (i.e., the torsion angle of the aneurysm to the upstream part of the parent artery).Imai et al [5] analyzed the steady-state inflow for aneurysms created at U-shaped, twisted, and S-shaped arteries and results suggest that the arterial geometry and secondary flow should be considered in the design of endovascular devices. K Sato et al. [6] performed simulation on models including parameters for parent artery shape and configuration of the aneurysm in parent artery.

Several works have been done on the treatment of aneurysm by stenting. Hassan et al. [7] discussed about the effect of placing single and double stent in the circumferential pressure distribution and concluded that aneurysm was adversely affected due to stent deployment and also suggested to keep in mind to choose which group of aneurysm is the best candidate for such treatment strategy. Hyunkim et al. [8] performed numerical analysis on the effect of stent strut shape and porosity on the hemodynamic properties of the flow inside aneurysm. Babiker et al. [9] performed analysis on quantitative effects of coil packing density on aneurysm fluid dynamics by in vitro steady flow study.

Attempts have been taken for finding relation between geometry and rupture risk using parameters like size, aspect ratio [21, 24]. Maximum works have been done on changing the aneurysm height and neck width ratio. But K Sato et al. [6] proposed that there is significant change in different factors because of the change of aneurysm diameter and neck size ratio.

How risk varies with the change of the neck size for different particular neck shapes has not been discussed comparatively. In our simulation we will find out how the risk factors change with the change of the neck size for the circular and the elliptical neck.

2.Methodology:

The characteristics of flow inside the aneurysm mainly depends on the shape and size of the aneurysm as well as the parent artery. The flow varies greatly due to the change of shape and size of aneurysm dome and neck including parent artery diameter [10,5,11,3,12,6]. There is a trend of using patient-specific models in the analysis of blood flow in CFD [17,18,19,20]. However, we have considered idealized model because a parametric study using idealized model can clearly reveal the effect of geometric characteristics on inflow features [5].we have considered our geometry according to the theory described by Parlea et al.[14]

2.1. Geometry & Grid:

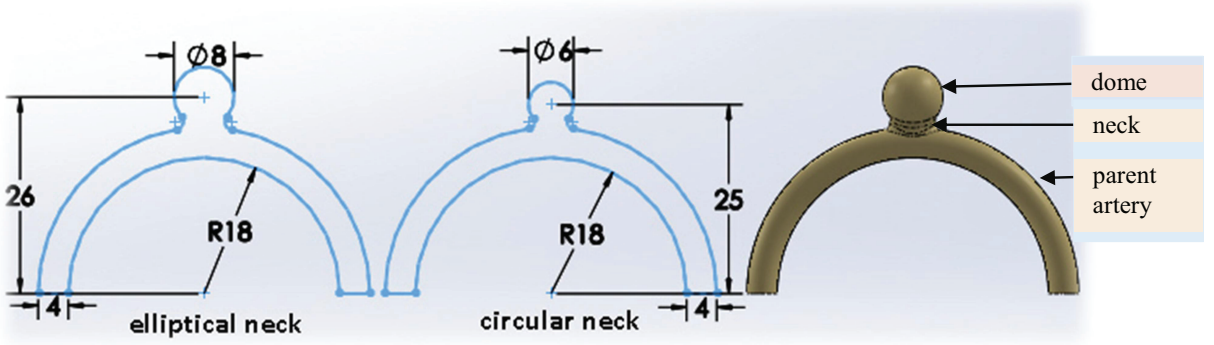

Figure 1: Aneurysm model

We have taken our aneurysm model geometry almost similar to the geometry described by G. Mulder et al. [2] we have changed the neck shape and size for four different models which are within the range described in Parlea et al. [14]. The models with their dimensions are presented in the table below.

Table 1: Aneurysm models with dimensions

Model	Elliptical neck			Circular neck	
	Major neck diameter (mm)	Minor neck diameter (mm)	Dome diameter (mm)	Neck diameter (mm)	Dome Diameter (mm)
Model 1	8			3.5	
Model 2	7			3	
Model 3	6	3.5	8	2.5	6
Model 4	5			2	

According to the meshing considered in Mulder et al. [2], we have taken the tetrahedral mesh for our models. Element size of .00025m and elements ranging 600000-1200000 have been taken. The results do not change appreciably if the element number is taken 1200000 or more. Advanced sizing functions have been applied on the curvature with high smoothing of the element.

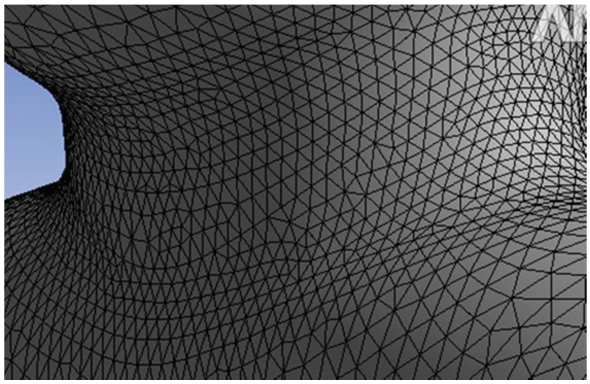

Figure 2: ANSYS meshing

2.2. Materials and Methods:

Sudo et al. [15] discussed about the fully developed oscillatory motion in a curved pipe. It was concluded that when the Dean number is less than or equal to 100 the pipe curvature effects can be neglected. They classified secondary flow in 5 groups and one of which is Dean circulation having Dean number less than or equal to 100 and Womersley number under 5.5. It was shown that the center of secondary flow vortex scarcely shifts during pulsatile cycle because the viscous effect moves to the center of the vessel (pipe) for having low Dean number and Womersley number. The Dean number of our model is approximately 100 and as the Womersley number in cerebral artery is less than 5, the pulsatile flow can be considered as steady laminar flow. However, consideration of pulsatile flow is most appropriate to describe the blood flow but it is computationally burdensome. So we considered the steady state laminar flow with average Reynolds number 330. The governing equations are the steady-state Navier–Stokes equation and the continuity equation.

$$\rho (u \cdot \nabla u) = -\nabla p + \mu \nabla^2 u \quad \ldots\ldots\ldots\ldots\ldots\ldots\ldots (1)$$

$$\nabla \cdot u = 0 \quad \ldots\ldots\ldots\ldots\ldots\ldots\ldots (2)$$

Where u is the flow vector, ρ is the density (kg/m^3), p is the pressure and μ is the dynamic viscosity (Ns/m^2).

Ku et al. [16] told that the Reynolds number ranges from 110 to 850 in large arteries so the non-Newtonian effect is not appreciable for blood. So neglecting the non- Newtonian effect we assumed blood to be the Newtonian incompressible fluid where the density is taken as 1008, flow rate in 4 mm parent artery is 3.6 mL/s, velocity magnitude is .2365 m/s and viscosity is .0035 N/m^2s^2.

The boundary condition which we have used are- no slip condition at the wall, inlet considered as velocity inlet having Poiseuille velocity profile and free pressure outlet. Reynolds number has been taken as 330 which is the average of the systolic and diastolic Reynolds number for normal human cerebral blood flow in artery. We used the ANSYS CFD FLUENT package for solving the problems. The ANSYS CFD FLUENT uses the finite volume method to solve the problems.

3. Validation:

With little geometric change flow properties vary a lot as described in Hoi et al. [12]. In Yi-sen et al. [11] the geometric parameters are well defined. So we have considered this paper as a reference to validate our paper.

Table 2: comparison of the results between Yi-sen et al. and our simulated value

Parameter	Value in Yi-sen et al.	Our simulated value
Maximum velocity (m/s)	0.2089	.23
Average velocity (m/s)	0.0550	0.052
WSS (Pa)	1.2351	1.23351

The chart above shows very minor difference between our simulated value and the value found from Yi-sen et al. [11]

Our result

Result from Yi-sen et al.

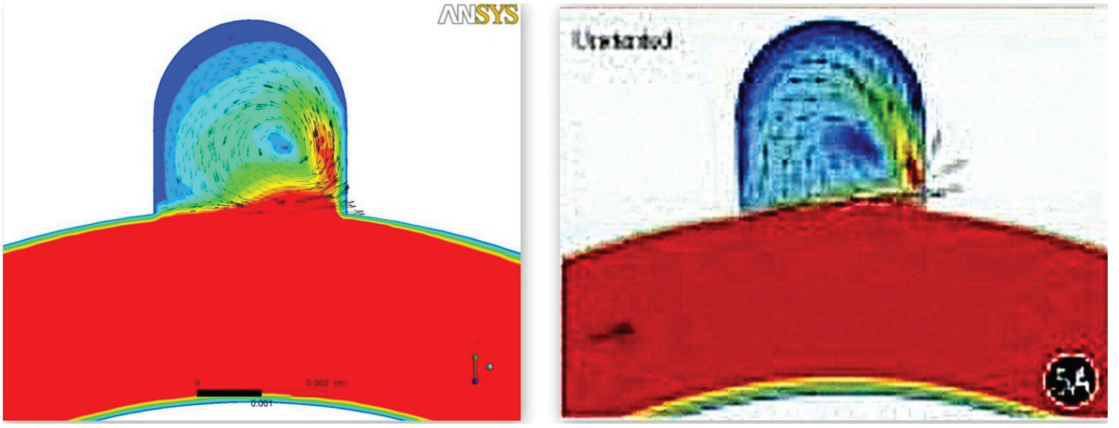

Figure 3: Flow profile in the unstented aneurysm model (5A) described in Yi-sen et al.

4. Results and Discussions:

For the result acquisition from the CFD simulation, we have considered two planes corresponding to plane a and b where plane a is the middle plane and plane b is the neck of the model. The two planes are shown in the figure.

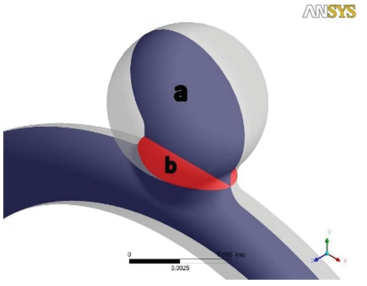

Figure 4: planes inside the aneurysm model

Elliptical neck *circular neck*

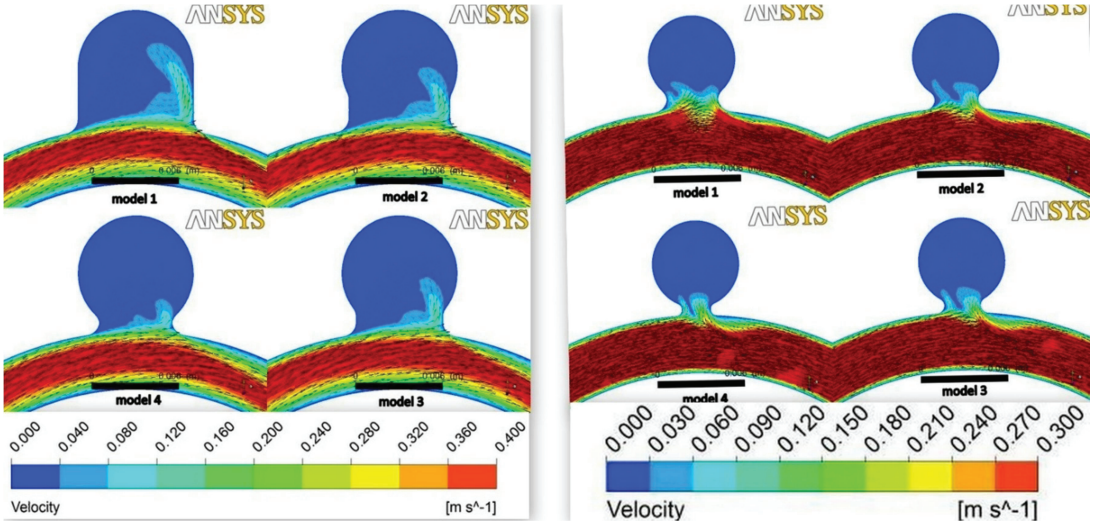

Figure 5: velocity vectors with contour in the middle plane (plane a of figure4) of the models. The left side is of each model is the upstream side and the right side is the downstream side.

For both elliptical neck and circular neck the velocity vector with the contour is shown. Here color in the legend (placed at the bottom) represents the velocity magnitude. The main flow from the parent artery strikes the neck at the downstream side and enters inside the aneurysm and eventually creates a vortex in the models with elliptical necks. No double vortices were found. But the flow from the main artery enters along the upstream side of the aneurysm and comes out of the dome along the downstream side for circular neck. In the elliptical neck, for model 1 the flow is more and creates a larger inflow contour and the flow gradually decreases for the model 2, model 3 and model 4 respectively. In the circular neck, for model 1, one smaller vortex was found at the proximal side of the neck along with the larger vortex. The flow pattern inside the other three models consisted of single vortex. The velocity magnitude and area of inflow gradually decreases in the model 2, model 3 and model 4 respectively.

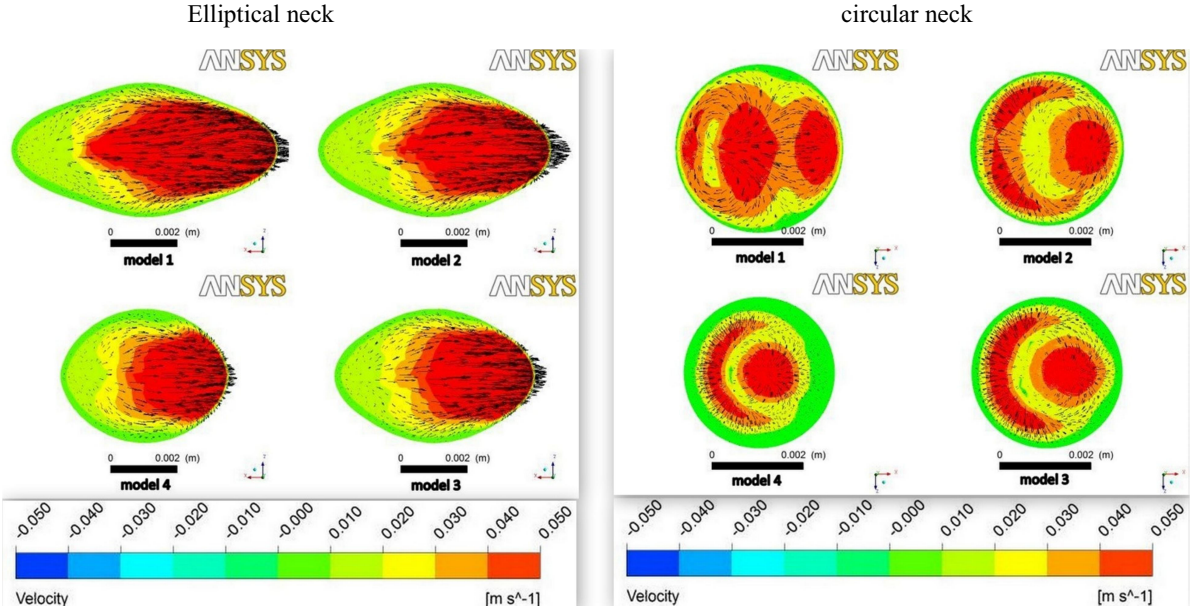

Figure 6: velocity vector (tangential) and contour in the neck (plane b of figure4). The main flow in the artery is from left to right. The view of the neck is from the top side of the aneurysm.

In the elliptical neck sections, in the model 1 the higher velocity vector with higher inflow area is found to enter inside the aneurysm (vectors coming out perpendicular to the plane) along the distal side compared to other models. And the outflow (vectors going inside perpendicular to the plane) of the blood is along the proximal side of the neck. The magnitude and the area of inflow decrease in the models 2, 3 and 4 gradually. And for the circular neck, for model 1, the left two red sections indicate the blood inflow to the aneurysm and the right red section indicates the blood outflow. The flow in model 1 occurs with higher area. For the other three models, the left crescent section indicates the area of inflow and the right circular section indicates the area of outflow. The area decreases in models 2, 3 and 4 gradually.

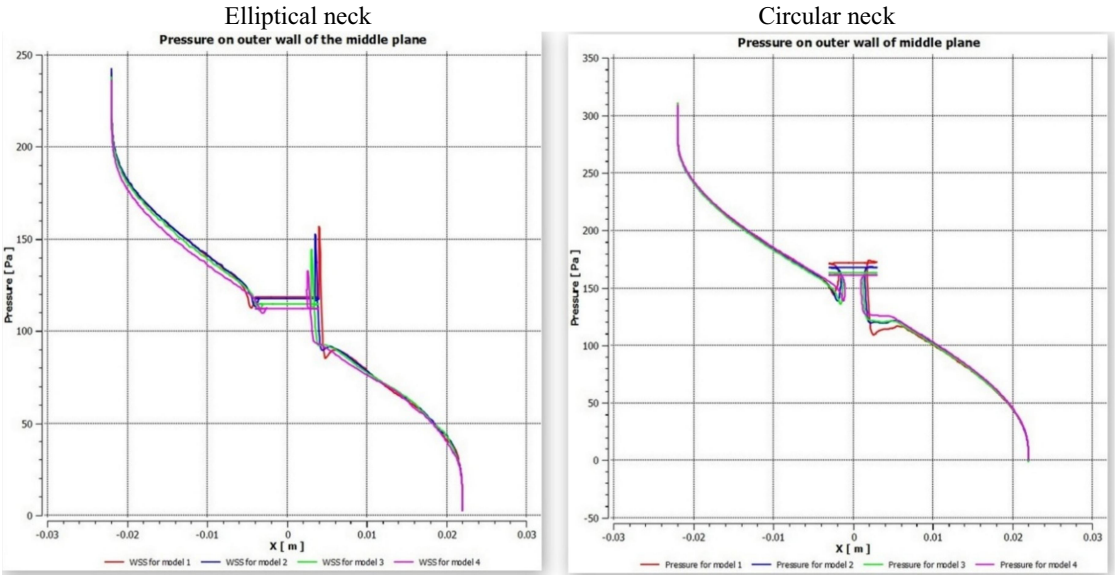

Figure 7: Pressure distribution on the outer wall of the middle plane (plane a in figure 4) along the line from inlet to outlet. X=-0.022 is the inlet section and x=.022 is the outlet section.

We have taken the pressure distribution along a polyline on the outer wall of the middle plane. Here the proximal sections of the necks for the models are within x=-.004 to -.001m and the distal section of the necks are within x=.001 to .004m. From the graph of the elliptical neck it is seen that the pressure slightly reduces at the proximal section of the neck and remains almost constant inside the dome and abruptly increases at the distal section of the neck. The magnitude of the pressure reduces from model 1 to model 4 gradually. In case of circular neck, pressure reduces at proximal section and abruptly increases and remains constant inside the dome and then decreases.

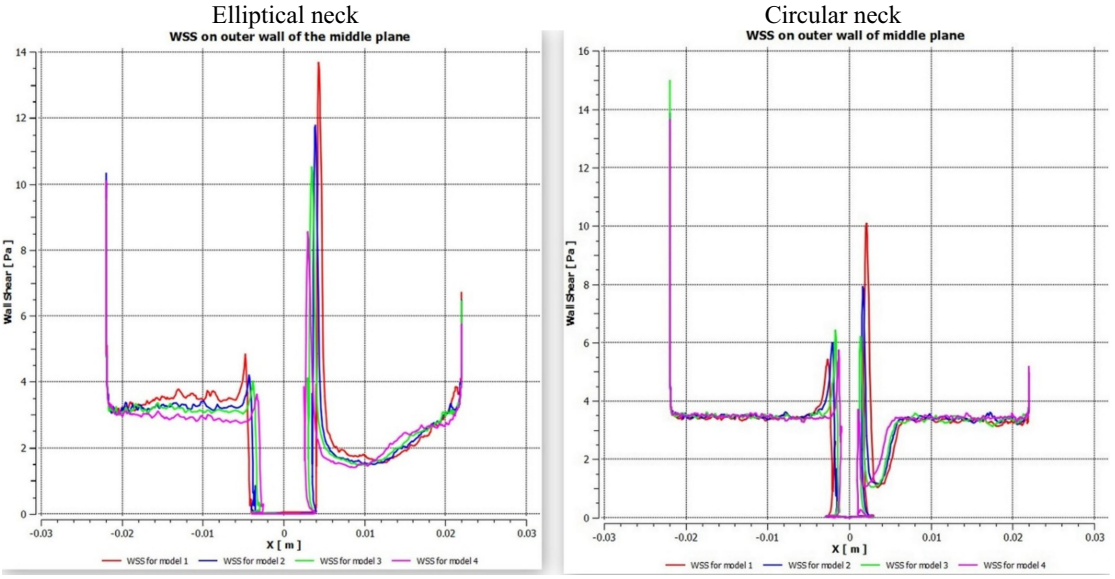

Figure 8: wall shear stress (WSS) distribution on the outer wall of the middle plane (plane a in figure 4) along the line from inlet to outlet. x=-.022 is the inlet section and x=.022 is the outlet section.

Same as pressure, we have simulated the WSS distribution along the polyline on the outer wall of the middle plane. The proximal section of the neck are within x=-.004 to -.001m and the distal section of the necks are within x=.001 to .004m. The wall shear stress increases slightly at the proximal neck and the increase is higher at the distal neck. The blood during inflow to and outflow from the dome strikes the proximal neck and the distal neck creating higher wall shear stress. In comparison to the proximal neck the WSS in the distal neck is lot more which indicates higher rupture risk at the distal neck. And the WSS on the walls of the aneurysm decreases in the sequence of 1, 2, 3 and 4.

Here we have presented different parameters for different models for both elliptical and circular neck separately.

Table 3: Different parameter in the aneurysm of the middle plane (plane a in figure 4) for elliptical neck:

Model	Average velocity(m/s)	Maximum velocity(m/s)	Average pressure(Pa)	Maximum pressure(Pa)	Average WSS(Pa)	Maximum WSS(Pa)
Model 1	0.0483	0.330	120.455	157.0	1.5215	13.70
Model 2	0.0443	0.290	119.555	153.0	1.4865	11.78
Model 3	0.0404	0.250	116.208	144.8	1.4408	10.53
Model 4	0.0300	0.225	113.153	133.4	0.9338	8.55

Table 4: Different parameter in the aneurysm of the middle plane (plane a in figure 4) for circular neck:

Model	Average velocity(m/s)	Maximum velocity(m/s)	Average pressure(Pa)	Maximum pressure(Pa)	Average WSS(Pa)	Maximum WSS(Pa)
Model 1	0.0260	0.310	170	175.508	1.094	10.09
Model 2	0.0210	0.236	166	171.450	0.858	7.93
Model 3	0.0195	0.199	161	165.348	0.791	6.23
Model 4	0.0190	0.195	159	161.270	0.740	5.23

5. Conclusion:

From the above study, it is seen that for both elliptical and circular neck aneurysms the parameters like velocity, pressure, wall shear stress increase with the increase of the neck size. And the rupture risk is directly related to those parameters. So it can be concluded that “the rupture risk increases with the increase of size of the aneurysm neck for both elliptical and circular neck aneurysms provided that the aneurysm has got fixed dome diameter”.

6. Reference:

[1] Weir, B. Unruptured intracranial aneurysms: a review,J. Neurosurg.96:3–42, 2002.

[2] Gwen Mulder, Arjen C. B. Bogaerds,Peter Rongen,Frans N. van de Vos, On automated analysis of flow patterns in cerebral aneurysms based on vortex identification, J Eng Math (2009) 64:391–401,DOI 10.1007/s10665-009-9270-6.

[3] Yiemeng Hoi, M.S., Hui Meng, Ph.D., Scott H. Woodward, M.S.,Bernard R. Bendok, M.D., Ricardo A. Hanel, M.D.,Leer. Guterman, Ph.D., M.D., Nelson Hopkins, M.D., Effects of arterial geometry on aneurysm growth: three dimensional computational fluid dynamics study, J Neurosurg 101:676–681, 2004.

[4] Kodai Sato, Yohsuke Imai, Takuji Ishikawa, The importance of parent artery geometry in intra aneurysmal hemodynamics, Medical Engineering & Physics 30 (2008) 774–782.
[5] Yohsuke Imai,Kodai Sato,Takuji Ishikawa, And Takami Yamaguchi, Inflow into Saccular Cerebral Aneurysms at Arterial Bends, Annals of Biomedical Engineering, Vol. 36, No. 9, September 2008 (2008)pp. 1489–1495, DOI: 10.1007/s10439-008-9522-z.
[6] Kodai Sato, Yohsuke Imai, Takuji Ishikawa,Noriaki Matsuki, Takami Yamaguchi, The importance of parent artery geometry in intra-aneurysmal hemodynamics, Medical Engineering & Physics 30 (2008) 774–782.
[7] Tamer Hassan&Yasser Mohamed Ahmed&Amr Ali Hassan, The adverse effects of flow-diverter stent-like devices on the flow pattern of saccular intracranial aneurysm models: computational fluid dynamics study,
[8] Yong Hyunkim,Xiaofeng Xu,And Joon Sang Lee, The Effect of Stent Porosity and Strut Shape on Saccular Aneurysm and its Numerical Analysis with Lattice Boltzmann Method, Annals of Biomedical Engineering, Vol. 38, No. 7, July 2010 (2010)pp. 2274–2292, DOI: 10.1007/s10439-010-9994-5.
[9] M.Haithem Babiker,L.Fernando Gonzalez,Felipe Albuquerque,Daniel Collins,Arius Elvikis,And David H. Frakes, Quantitative Effects of Coil Packing Density on Cerebral Aneurysm Fluid Dynamics: An In VitroSteady Flow Study, Annals of Biomedical Engineering, Vol. 38, No. 7, July 2010 (2010)pp. 2293–2301,DOI: 10.1007/s10439-010-9995-4.
[10] Hiroshi Ujiie, Chie Shinohara, Takashi Higa, Koichi Kato, Shigeka Yoshimoto, Tomokatsu Hori, Intraaneurysmal flow and aspect ratio (dome/neck), J Biorheol (2009) 23:41–48,DOI 10.1007/s12573-009-0006-z.
[11] ZHANG Yi-sen, YANG Xin-jian, WANG Sheng-zhang, QIAO Ai-ke, CHEN Jia-liang, ZHANG Kun-ya, LIU Zhi-cheng, ZHAO Yu-jing, ZHANG Ying, LUO Bin and LI Chuan-hui, Hemodynamic effects of stenting on wide-necked intracranial aneurysms, Chinese Medical Journal 2010;123(15):1999-2003.
[12] Yiemeng Hoi, Scott H. Woodward, Minsuok Kim, Dale B. Taulbee, Hui Meng, Validation of CFD Simulations of Cerebral Aneurysms With Implication of Geometric Variations, J Biomech Eng. 2006 December ; 128(6): 844–851. doi:10.1115/1.2354209.
[13] Ryuhei Yamaguchi · Hiroshi Ujiie · Sayaka Haida Nobuhiko Nakazawa · Tomokatsu Hori, Velocity profile and wall shear stress of saccular aneurysms at the anterior communicating artery, Heart Vessels (2008) 23:60–66, DOI 10.1007/s00380-007-0996-7.
[14] Luciana Parlea, Rebecca Fahrig, David W. Holdsworth, and Stephen P. Lownie, An Analysis of the Geometry of Saccular Intracranial Aneurysms, AJNR Am J Neuroradiol20:1079–1089, June/July 1999.
[15] K. Sudo, M. Sumida, R. Yamane, Secondary motion of fully developed oscillatory flow in a curved pipe, J. Fluid Meeh. (1992), vol. 237, pp. 189-208.
[16] Ku, J. P., C. J. Elkins, and C. A. Taylor. Comparison of CFD and MRI flow and velocities in an in vitro large artery bypass graft model. Ann. Biomed. Eng. 33:257–269,2005. doi:10.1007/s10439-005-1729-7
[17] Castro, M. A., C. M. Putman, and J. R. Cebral. Computational fluid dynamics modeling of intracranial aneurysms: effect of parent artery segmentation on intra-aneurysmal hemodynamics.Am. J. Neuroradiol.27:1703–1709, 2006.
[18] Cebral, J. R., and R. Lo¨hner. Efficient simulation of blood flow past complex endovascular devices using and adaptiveembedding technique.IEEE Trans. Med. Imaging24:468–476, 2005. doi:10.1109/TMI.2005.844172.
[19] Steinman, D. A., J. S. Milner, C. J. Norley, S. P. Lownie, and D. W. Holdsworth. Image-based computational simulation of flow dynamics in a giant intracranial aneurysm. Am. J. Neuroradiol.24:559–566, 2003.
[20] Torii, R., M. Oshima, T. Kobayashi, K. Takagi, and T. E.Tezduyar. Influence of wall elasticity in patient-specific hemodynamic simulations. Comput. Fluids 36:160–168, 2007. doi:10.1016/j.compfluid.2005.07.014.
[21] Gonzalez CF, Cho YI, Ortega HV, et al: Intracranial aneurysms: flow analysis of their origin and progression. AJNR 13:181–188,1992
[22] Kassell NF, Torner JC: Size of intracranial aneurysms. Neurosurgery 12:291–297, 1983
[23] Parlea L, Fahrig R, Holdsworth DW, et al: An analysis of the geometry of saccular intracranial aneurysms. AJNR 20:1079–1089,1999
[24] Ujiie H, Tamano Y, Sasaki K, et al: Is the aspect ratio a reliable index for predicting the rupture of a saccular aneurysm? Neurosurgery 48:495–503, 2001